J Therm Anal Calorim (2016) 126:733–742
DOI 10.1007/s10973-016-5527-2

TG–MS study on the effect of multi-walled carbon nanotubes and nano-Fe_2O_3 on thermo-oxidative stability of silicone rubber

Zhe Wang[1] · Hongyan Li[1] · Junping Zheng[1]

Received: 31 July 2015 / Accepted: 11 May 2016 / Published online: 25 May 2016

Abstract In this work, an investigation was focused on how carbon nanotubes and nano-Fe_2O_3 improved the thermo-oxidative stability of silicone rubber (SR). A series of nanoparticles, including carbon nanotubes (CNTs), Fe_2O_3 with two different crystalline forms (α-Fe_2O_3 and γ-Fe_2O_3), a mixture of CNTs and γ-Fe_2O_3 (γ-Fe_2O_3 + CNTs), and γ-Fe_2O_3-modified CNTs (γ-Fe_2O_3 − CNTs), were involved in this article. Thermal degradation characteristics of SR samples filled with these nanoparticles were investigated through thermogravimetric analysis equipped with mass spectroscopy system (TG–MS), and the evolutions of prominent volatiles corresponding to different stages of decomposition were recorded. It was discovered that these nanoparticles affected the thermo-oxidative stability of SR in different ways. While CNTs had an effect of delaying every stage of the degradation of silicone rubber, Fe_2O_3 inhibited the oxidation of the side methyl, in which γ-Fe_2O_3 had better performance. γ-Fe_2O_3 − CNTs had the best effect on preventing the side methyl from degradation, which can be seen from the remarkable decreases in methanol, methanoic acid and methane by 58.91, 57.27 and 27.45 %, respectively. This effect was superior to CNTs, γ-Fe_2O_3 or a mixture of both at the same addition amount. Herein, the reason for the different performance of these nanoparticles, which make a profound contribution to further improvement in thermo-oxidative stability of SR, has been discussed.

✉ Junping Zheng
jpzheng@tju.edu.cn

[1] Tianjin Key Laboratory of Composite and Functional Materials, School of Materials Science and Engineering, Tianjin University, Tianjin 300072, People's Republic of China

Keywords Thermo-oxidative stability · Mass spectroscopy · Carbon nanotubes · Iron oxides · Silicone rubber

Introduction

Silicone rubber (SR) is one of the most studied high-performance synthetic rubbers being used in high-temperature environment, which must be attributed to its excellent thermo-oxidative stability over conventional carbon backbone rubbers [1, 2]. The extraordinary thermo-oxidative stability of SR derives from its unique backbone structure of Si–O chemical bond, whose bond energy (451 kJ mol^{-1}) is much higher than that of common C–C chemical bond (345 kJ mol^{-1}). With the rapid development of science and technology, the demand for better thermal resistant SR is increasing day by day [3, 4]. In the past several decades, lots of methods have been applied to improve the thermo-oxidative stability of SR [5–8]. Among them, adding thermal resistant additives into SR matrix is the most common one.

For further improvement in the thermo-oxidative stability, study of the roles thermal resistant additives play in SR matrix is in great request. Fe_2O_3 has been widely investigated as a traditional and effective thermal resistant one, and several theories have been proposed to demonstrate how it improves the thermo-oxidative stability of SR. Wilson's results [9] indicated that it was the bonding of rubber chains to the surface of Fe_2O_3 particles that prevented the formation of volatile oligomers and added stabilizing cross-linkings to the network. Since discovered in 1991 [10], carbon nanotubes (CNTs) have also attracted attentions [11, 12]. In the past few years, embedding CNTs into silicone rubber matrix has also been a hot topic [13–15]. Some of the researchers have been focused on the

thermal stability, and several theories have also been proposed to explain the action mechanism. Watts et al. thought CNTs may interrupt radical chain reaction of thermo-oxidative decomposition of silicone rubber, leading to antioxidant effects in polymeric materials [16]. Shen et al. considered that CNTs in the composite acted as radical scavengers, delaying the onset of thermal degradation and hence improving the thermal stability of the polymers [17]. However, these theories were mostly proposed on the basis of the macroscopic properties that composites exhibited in tests, and few reports have given direct evidence of their inferences how nanoparticles like Fe_2O_3 or CNTs affect the degradation process of SR.

Efforts have been paid to reveal the process of SR thermal degradation since 1980s, and up to now, the mechanism is quite mature. Thermal degradation of SR in air can be divided into three stages: thermal oxidation of side methyl, bond breaking of side methyl and depolymerization of backbone, as shown in detail in Scheme 1 [18–20]. Depolymerization of the backbone is a quite complex reaction which differs with different end groups of the backbone [20]. The SR used in our research is end-capped with inert groups; thus, the main backbone reaction during the degradation is the random scission reaction which mainly results in the formation of small cyclic products of siloxane. Our previous work [21] has confirmed that CNTs and different crystalline forms of Fe_2O_3 have varying degrees of the effects on thermo-oxidative stability of SR. What is more, the effect of Fe_2O_3-modified CNTs (γ-Fe_2O_3 − CNTs) was superior to any single thermal resistant additive. However, in which stage Fe_2O_3 or CNTs affect the degradation process of SR and to what extent they affect the thermo-oxidative degradation process have not been studied yet. Therefore, there is still a great need to make a comprehensive and thorough study on how they improve the thermo-oxidative stability of SR. This kind of study requires the identification and quantification of products simultaneously with the thermal decomposition, and one of the best techniques that can accomplish these requirements is the thermogravimetric analysis coupled to mass spectrometry (TG–MS) [22–25]. It provides quantitative results regarding the evolution of volatiles as a function of temperature. In this way, TG–MS measurement gives basic information about subtle chemical microstructure changes in SR-based composite during thermal degradation process and makes a significant contribution to mechanism study.

In this study, as a continuation of our previous work, a series of SR samples concerning five different kinds of nanoparticles were involved to investigate the effects these nanoparticles had on the thermo-oxidative stability of SR matrix. TG–MS analysis was performed, and the evolution of volatiles was recorded, which can give a direct reflection of subtle chemical microstructure changes during the degradation process. Based on the evolution of volatiles, how these nanoparticles affect the thermo-oxidative stability are revealed, and several possible reasons for the synergistic effect are proposed.

Experimental

Materials

Methylvinyl silicone gum (110-2; Mn, $5.0 \times 10^5 \sim 7.0 \times 10^5$; vinyl group content, 0.15 ~ 0.18 mol%) was purchased from Bluestar Chengrand Chemical Co. Ltd.(Chengdu, China). Carboxylic CNTs (carboxyl ratio 2.31 mass%; purity >95 %; diameter 20–40 nm; length 1–2 μm) were purchased from Shenzhen Nanotech Port Co. Ltd., China. Fumed silica (AS-380) was purchased from Shenyang Chemical Co. Ltd. (China). Hexamethyldisilazane, polyvinylsilicone oil and 2,5-bis(tertbutylperoxy)-2,5-dimethylhexane (DBPMH) were all industrial products and used as received. Other reagents were all of analytical reagents.

Preparation of γ-Fe_2O_3 − CNTs

$Fe(NO_3)_3 \cdot 9H_2O$ (1.50 g) was added into 200 mL of absolute ethanol and stirred until it was dissolved completely. This solution was added 0.35 g of carboxylic CNTs, stirred and sonicated for 3 h. 0.08 g of sodium dodecylbenzenesulfonate was added into the solution, the mixture was stirred, and then 24 mL of ammonia solution was added as a gelation agent and stirred. The mixture was filtered and washed by a large amount of deionized water and then vacuum-dried at 60 °C for 72 h. The calcination of this powder was performed at 600 °C in a muffle furnace under argon atmosphere for 5 h and then annealed. γ-Fe_2O_3-modified CNTs was obtained and named as γ-Fe_2O_3 − CNTs.

Preparation of α-Fe_2O_3 and γ-Fe_2O_3

Preparation of α-Fe_2O_3 followed the same experimental method as that of γ-Fe_2O_3 − CNTs in the absence of CNTs. To obtain γ-Fe_2O_3, α-Fe_2O_3 was calcined at 400 °C for 0.5 h under hydrogen atmosphere [the α-Fe_2O_3 was changed to Fe_3O_4 ($FeO \cdot Fe_2O_3$)] and then at 300 °C for 3 h under air atmosphere (the Fe_3O_4 was changed to γ-Fe_2O_3).

Preparation of the other control particles

The obtained Fe_2O_3 and calcined CNTs were mixed under grinding. The mixture was named as Fe_2O_3 + CNTs which has a same mass ratio as that of Fe_2O_3/CNTs = 9:7

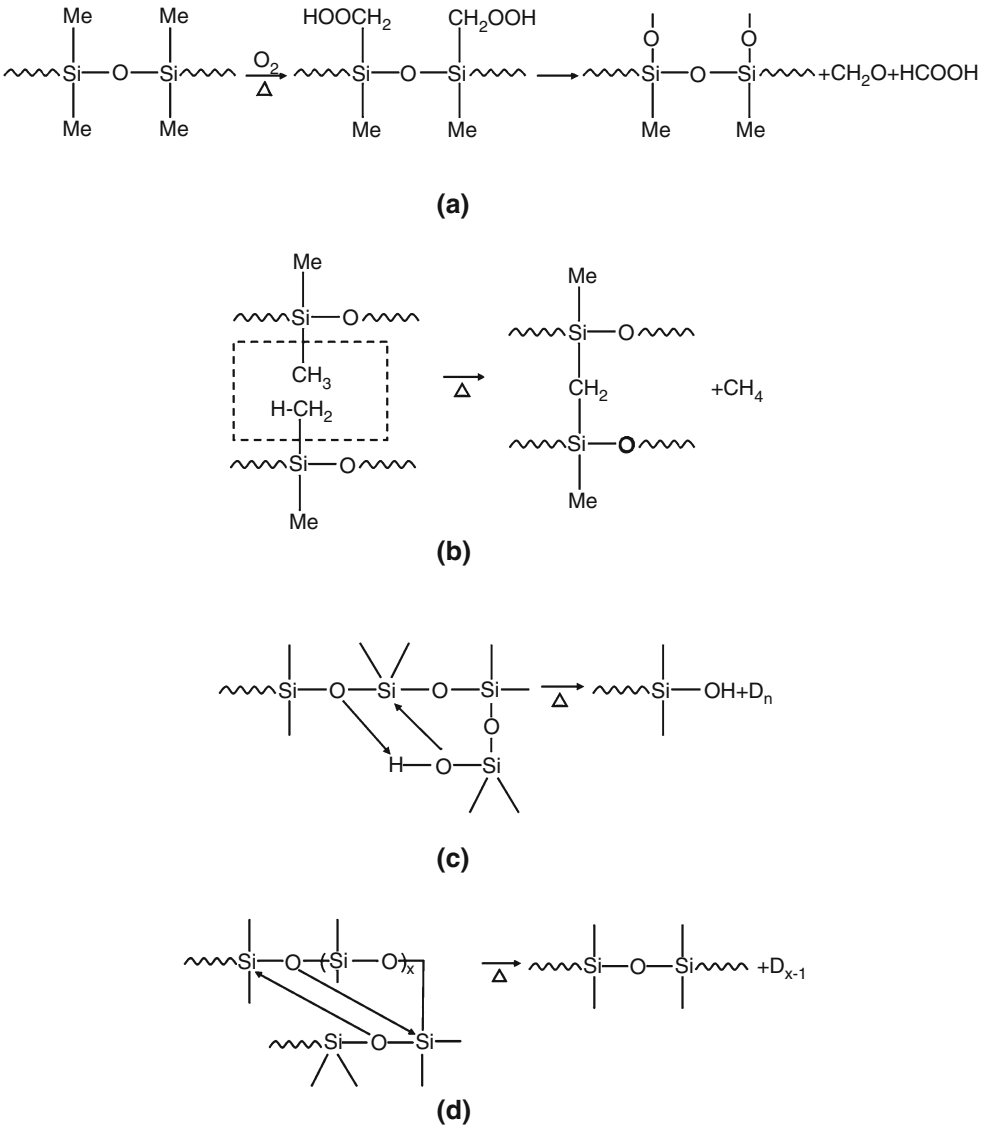

Scheme 1 Degradation steps of SR in air atmosphere. **a** Thermal oxidation of side methyl. **b** Bond breaking of side methyl. **c** and **d** are the depolymerization of backbone in different kinds of SR. **c** Unzipping reaction for SR containing silanol end groups. **d** Random scission reaction for SR end-capped with inert groups

(calculated from the reaction ratio) in the Fe_2O_3 − CNTs. Carboxylic CNTs was calcined at 600 °C in a muffle furnace under argon atmosphere for 5 h and then annealed, which was used as a control additive.

Preparation of silicone rubber-based composites

Materials were milled on a two-roll mill (SR-160B, Guangdong Zhanjiang Machinery Factory, China). Hundred phr (parts per hundreds of rubber) of silicone gum was encapsulated onto rollers. Forty phr of fumed silica, 10 phr of hexamethyldisilazane and 2.6 phr of polyvinylsiloxane were mixed step by step. Then, 3 phr of the prepared particles was added, respectively. After being milled uniformly, DBPMH was added as cross-linking agent. The mixture was cured in a stainless steel mold at 180 °C under a pressure of 10 MPa for 10 min and postcured at 200 °C for 4 h under ambient pressure for cross-linking.

Characterization

Thermogravimetric analysis (TG) was carried out using a Rigaku TA-50 instrument (Japan). About 10 mg of samples cut as small pieces was heated to 750 °C at a heating rate of 10 °C min^{-1} under air atmosphere.

In order to study the ways how CNTs, different crystalline forms of Fe_2O_3, and γ-Fe_2O_3 − CNTs improve the thermo-oxidative stability of SR composites, TG–MS analysis was performed with QMS 403/5 Skimmer (Netzsch, Germany) in air atmosphere. About 10 mg of samples cut as small pieces was decomposed with TG at a heating rate of 10 °C min^{-1} from ambient temperature up to

900 °C. The evolved volatiles were introduced to the mass spectrometer (MS) to obtain the real-time evolution curves of prominent volatiles.

Results and discussion

TG results analysis

To investigate the improvement effect of the nano-fillers involving CNTs and nano-Fe_2O_3, thermo-oxidative behaviors of blank SR and SR-based composites were evaluated by thermogravimetric analysis experiment. Figure 1 shows the TG and DTG curves of the samples in air at a heating rate of 10 °C min^{-1}. It can be seen that the degradation of samples in air can be generally divided into two overlapped steps according to the DTG curves which are not smooth with a lot of small peaks and fluctuations. Degradation of SR under air atmosphere can be classified into three different reactions as shown in Scheme 1, and depolymerization of backbone is the main reaction that occurs through the whole degradation process and results in the greatest amount of mass loss. The two-step feature of the process can be explained by the complicated coexistence of the three reactions. In general, the major degradation stages in most of the samples are the last peaks that appear above 520 °C in DTG curves, which are considered to be the characteristic peaks of the depolymerization of backbone. On the other hand, the first small peaks of samples all appearing between 361 and 416 °C are mainly contributed to the catalytic action of oxygen in the depolymerization process of SR to volatile cyclic oligomers. But it must be pointed out that the thermal oxidation of side methyl also has an important effect on the formation of small peaks.

From the TG curves of the samples, it can be observed that the γ-Fe_2O_3 − CNTs had the most positive effect on thermo-oxidative stability among all the samples, whose degradation curve is clearly postponed. This can also be confirmed by the DTG curves in which the major degradation peak of γ-Fe_2O_3 − CNTs sample appeared at the highest temperature. What can also be clearly observed in the DTG figure is the significant peak of the blank sample, because the peak intensity of the major peak is nearly twice as strong as the others. It proves that the degradation of blank sample is extremely drastic that happened in a rapid way.

Prominent products and characteristic data got from TG–MS

TG–MS is one of the most commonly used thermal analysis methods for polymer degradation. In the test, evolved volatiles from the composites decomposed with TG are introduced to MS. Thus, characteristic products produced by the degradation reactions of polymer can be identified. What is more, intensities of volatiles as a function of temperature can also be recorded by MS. Thus, curves of the evolution of volatiles can be drawn according to the data we got, and several characteristic points and values of each specific volatile can be obtained from the curves including T_0 (the temperature at which the volatile first detected), T_P (the temperature at which the peak of volatile evolution appeared) and I (the peak intensity of the volatile evolution). In this way, the products and corresponding mechanisms at a certain temperature stage of thermo-oxidative degradation are directly revealed. The thermo-oxidative degradation of SR can be divided into three stages, and each stage has its own characteristic products.

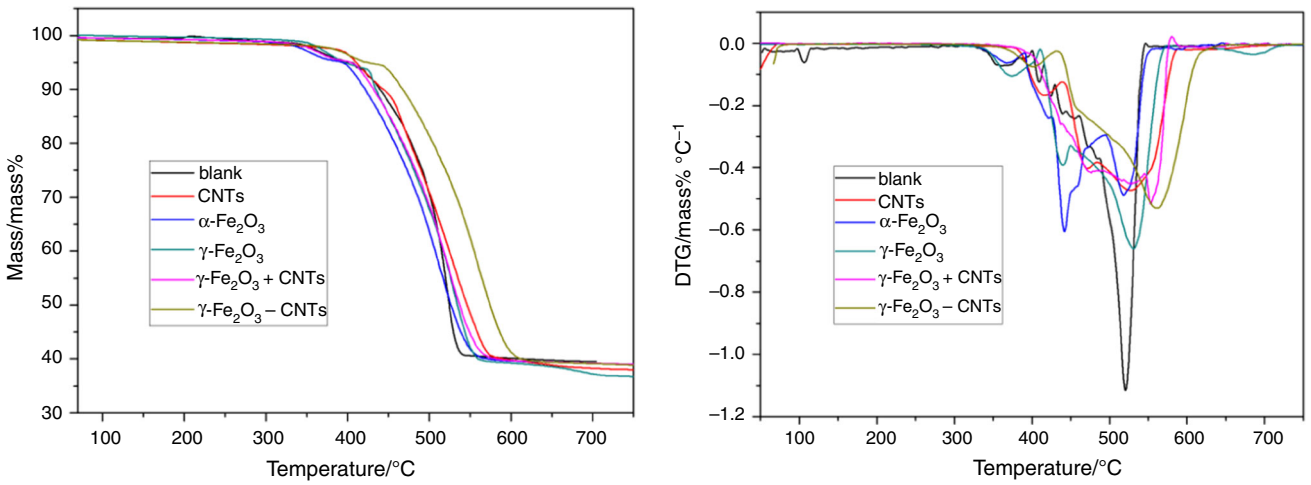

Fig. 1 TG and DTG curves of the samples in air at a heating rate of 10 °C min^{-1}

Table 1 Prominent products and corresponding mechanisms during the degradation process of SR

Product	Mechanism	Molecular formula	*m/z*
Methanol	Thermal oxidation of side methyl	CH_2O	30
Methanoic acid	Thermal oxidation of side methyl	HCOOH	46
Methane	Bond breaking of side methyl	CH_4	16
Hexamethylcyclotrisiloxane (D3)	Random scission of backbone	$C_6H_{18}O_3Si_3$	222
Octamethylcyclotetrasiloxane (D4)	Random scission of backbone	$C_8H_{24}O_4Si_4$	296
Decamethylcyclopentasiloxane (D5)	Random scission of backbone	$C_{10}H_{30}O_5Si_5$	370
Dodecamethylcyclohexasiloxane (D6)	Random scission of backbone	$C_{12}H_{36}O_6Si_6$	444

Prominent products and corresponding mechanisms during the degradation process of SR are shown in Table 1.

TG–MS analysis in air was performed for all samples including a blank sample and five kinds of composites mentioned above. The evolutions of volatiles corresponding to these samples are shown from Figs. 2–7, while characteristic points and values for the evolution of prominent volatiles in degradation identified by MS are summarized in Table 2.

Evaluation of the TG–MS curves of the blank and CNTs/SR samples

Evolutions of prominent volatiles of the blank sample are shown in Fig. 2. Methanol and methanoic acid are considered to be characteristic products from the oxidation of the side methyl. With temperature rising, oxidation of the side methyl got started. T_0 of methanol and methanoic acid were 211 and 235 °C, and T_P were observed at 417 and 423 °C, respectively. The bond breaking of side methyl took place at higher temperature stage. T_0 of the representative methane was about 327 °C, and T_P was observed at 437 °C. The evolutions of volatiles are consistent with the two stages of the degradation of side methyl. The oxidation of the side methyl took place earlier, while the bond breaking of it took place at higher temperature stage.

As can be seen in Fig. 2, the random scission reaction of the backbone took place later than the degradation of side methyl. D3, D4, D5 and D6, which are considered to be main products of the backbone reaction, were first detected at 278, 246, 318 and 406 °C and reached maximum at 543, 496, 511 and 595 °C, respectively. The formation of cyclic siloxane is affected by factors such as temperature, movement of molecule chain, steric hindrance. Theoretically speaking, D4 and D5 are the most stable kinds of cyclic siloxane. Thus, D4 and D5 are the most likely ones to be formed in the random scission of the backbone. With the number of chain units increasing, the likelihood of the cyclization decreases. So the formation of D6 happens later, and cyclic siloxanes with even more chain units are

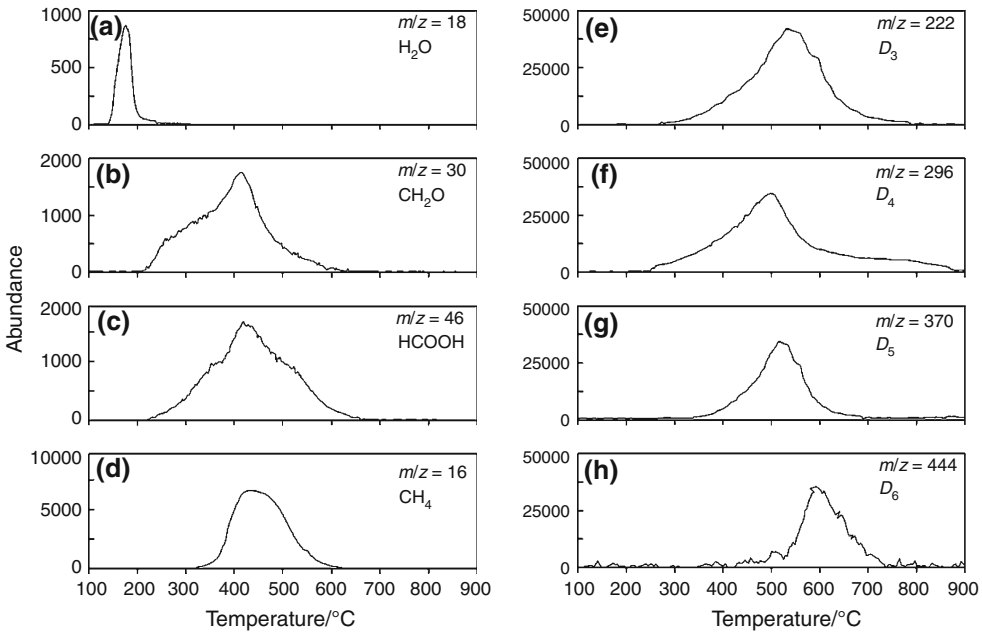

Fig. 2 Evolutions of prominent volatiles of the blank sample in air at 10 °C min^{-1}

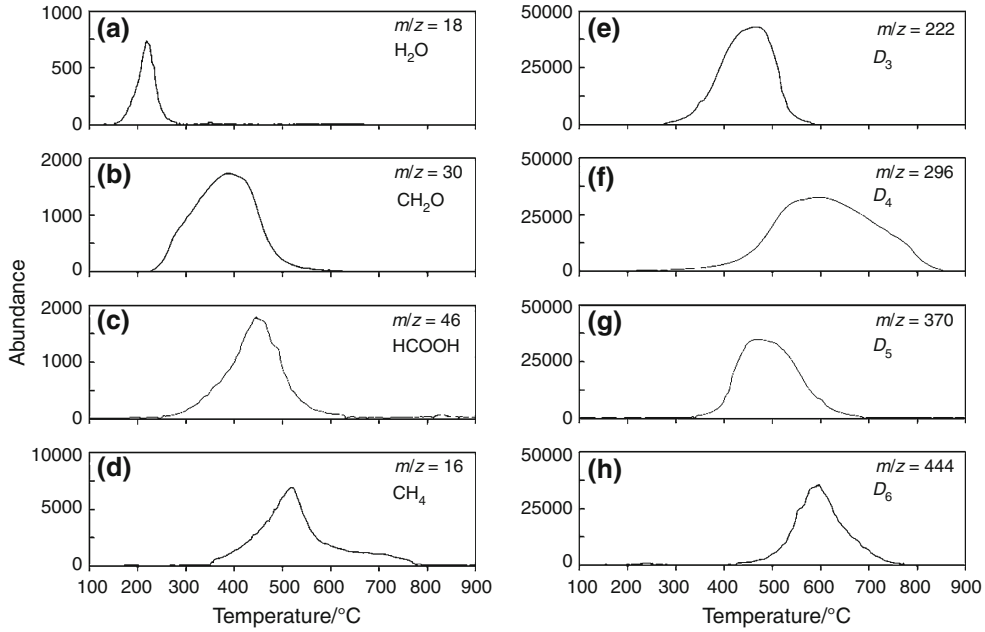

Fig. 3 Evolutions of prominent volatiles of CNTs/SR sample in air at 10 °C min^{-1}

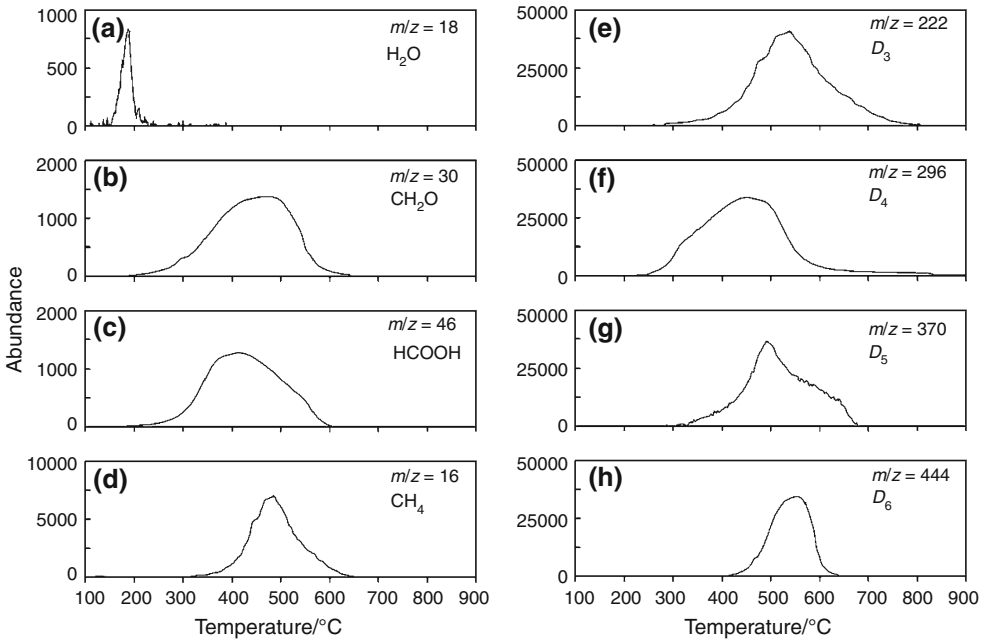

Fig. 4 Evolution of prominent volatiles of α-Fe_2O_3/SR in air at 10 °C min^{-1}

hard to form. Although D3 have the minimum amount of siloxane chain units, the large tension in cyclization process impede the formation.

From data we got, D4 was the one first detected. The following sequence was D3, D5 and D6. This is little different from the theoretical analysis. D4 was first detected at a relatively low temperature, which is decided by the thermodynamic property itself. However, with the temperature increasing, it was D3 rather than D5 that came out immediately following D4. It may be caused by the difference between cross-linked SR and linear polysiloxane. Theoretical analysis mentioned above is based on linear polysiloxane. In a real-world situation, after the cross-linking reaction, molecular chains of SR were restrained by the cross-linked network, and thus, the random scission of the backbone was inhabited. As a consequence, cyclic siloxane with fewer chain units was more prone to form. So D4 which is both thermodynamically stable and having

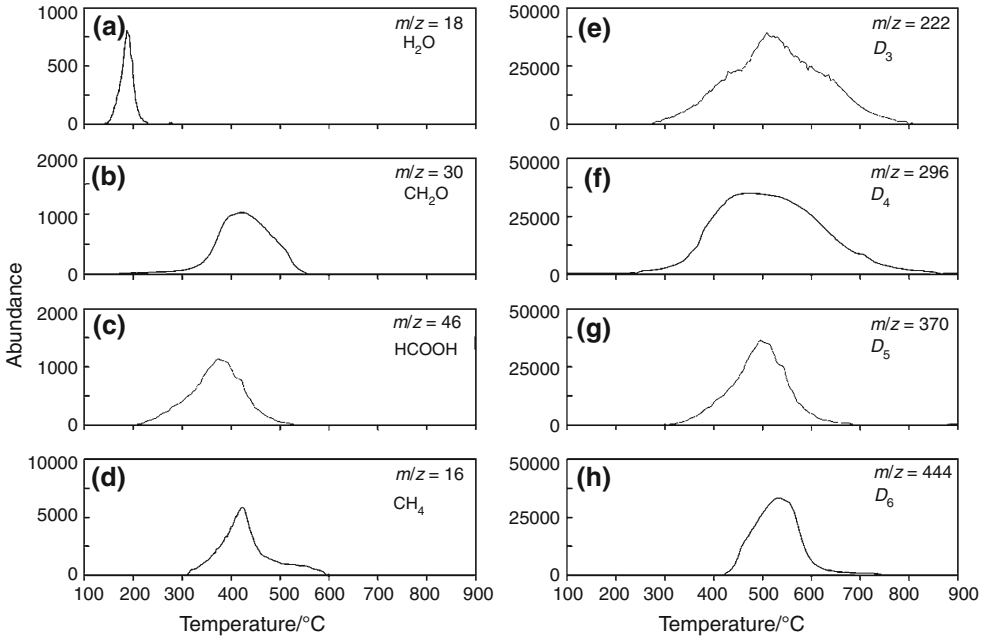

Fig. 5 Evolution of prominent volatiles of γ-Fe_2O_3/SR in air at 10 °C min^{-1}

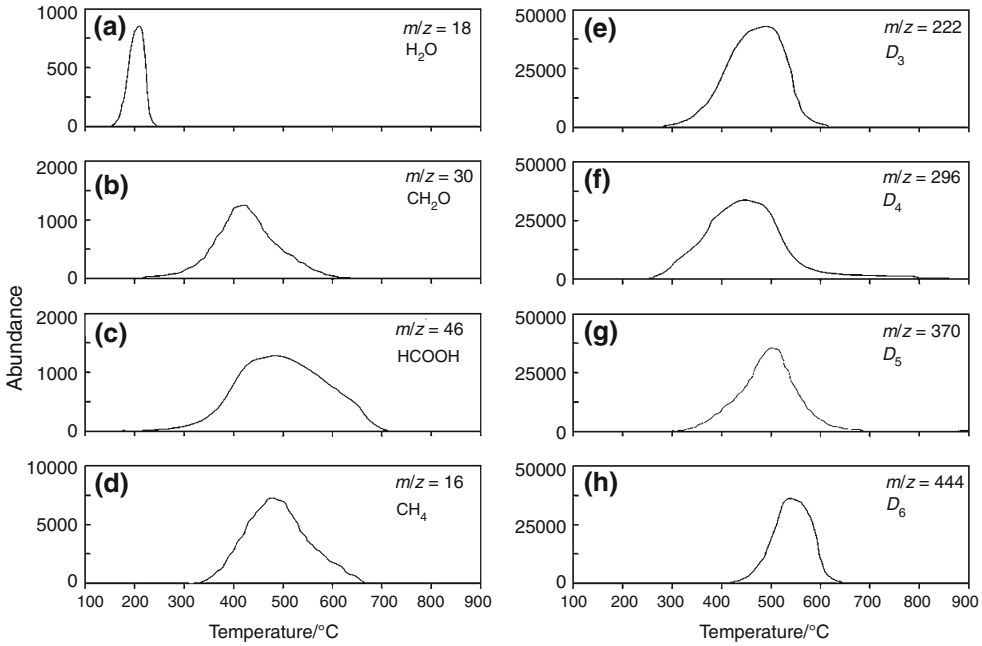

Fig. 6 Evolution of prominent volatiles of γ-Fe_2O_3 + CNTs/SR in air at 10 °C min^{-1}

fewer chain units came out first. Although D5 is more stable than D3 theoretically, the relatively more chain units make the chain segments of D5 hard to move and thus make it hard to form [26, 27]. So the formation of D3 is prior to D5.

Evolutions of prominent volatiles of CNTs/SR sample are shown in Fig. 3. Comparing with the data of blank sample, it can be discovered that T_0 of each volatile of CNTs/SR sample was higher than that of blank sample to varying degrees, which is consistent with the DTG curves. However, the peak intensity (I) of volatiles did not conform to this pattern. This phenomenon must be attributed to the presence of CNTs. CNTs have extremely high intrinsic thermal conductivity [28]. When added into SR matrix, thermal conductivity of composite was improved by CNTs, which had an effect of balancing the redundant heat in SR [29, 30]. In this way, the overheating of each specific section was restrained, so the degradation of SR was

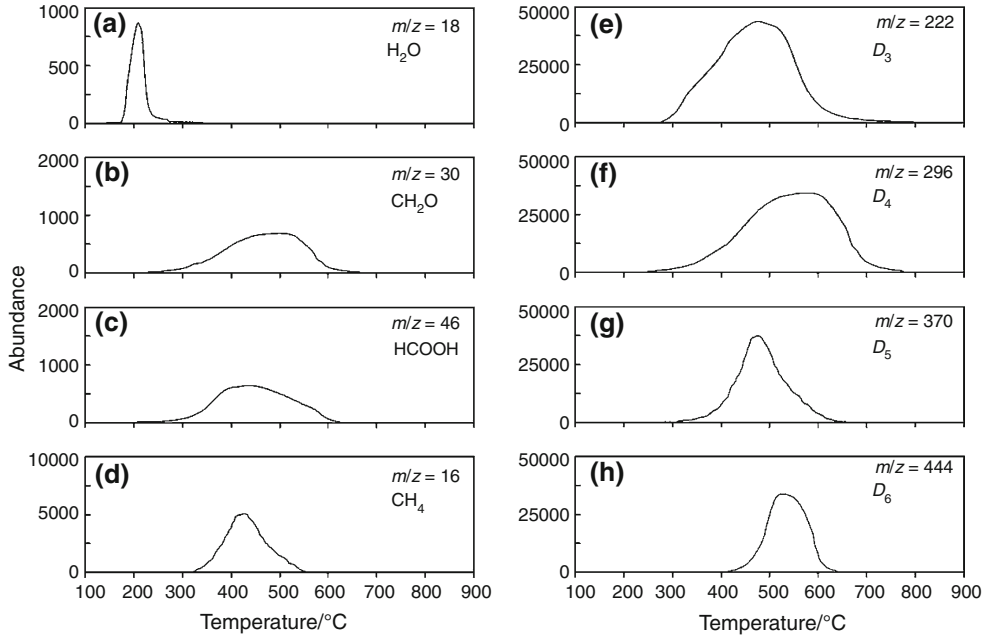

Fig. 7 Evolution of prominent volatiles of γ-Fe_2O_3 − CNTs/SR in air at 10 °C min^{-1}

Table 2 Characteristic points and values for the evolution of prominent volatiles in degradation identified by MS

Sample		CH_2O	HCOOH	CH_4	D3	D4	D5	D6
Blank	T_0/°C	211	235	327	278	246	318	406
	T_p/°C	417	423	437	543	496	511	595
	I (a.u.)	1.84×10^3	1.78×10^3	6.85×10^3	4.36×10^4	3.71×10^4	3.70×10^4	3.73×10^4
CNTs/SR	T_0/°C	232	253	345	285	262	336	413
	T_p/°C	386	441	528	473	573	482	596
	I (a.u.)	1.73×10^3	1.81×10^3	6.83×10^3	4.22×10^4	3.70×10^4	3.72×10^4	3.75×10^4
α-Fe_2O_3/SR	T_0/°C	185	210	320	282	247	321	411
	T_p/°C	463	404	496	537	458	496	563
	I (a.u.)	1.21×10^3	1.23×10^3	6.27×10^3	4.28×10^4	3.72×10^4	3.73×10^4	3.72×10^4
γ-Fe_2O_3/SR	T_0/°C	208	211	315	277	230	323	425
	T_p/°C	435	387	425	509	482	504	532
	I (a.u.)	1.10×10^3	1.15×10^3	5.24×10^3	3.95×10^4	3.72×10^4	3.73×10^4	3.72×10^4
γ-Fe_2O_3 + CNTs/SR	T_0/°C	223	237	331	280	261	320	411
	T_p/°C	417	478	470	488	452	499	549
	I (a.u.)	1.13×10^3	1.17×10^3	6.13×10^3	4.15×10^4	3.74×10^4	3.72×10^4	3.72×10^4
γ-Fe_2O_3 − CNTs/SR	T_0/°C	226	237	329	283	253	319	418
	T_p/°C	483	433	427	489	571	473	533
	I (a.u.)	7.56×10^2	7.61×10^2	4.97×10^3	4.26×10^4	3.67×10^4	3.76×10^4	3.69×10^4

T_0: the temperature at which the volatile was first detected

T_P: the temperature at which the peak of volatile evolution appeared

I: the peak intensity of the volatile evolution

postponed. When temperature increased to a certain threshold, the entire composite was overheated. Therefore, the excellent thermal conductivity of CNTs can no longer prevent SR from degradation, and the degradation took place in a rapid way. Because CNTs just played a role of balancing the redundant heat in SR matrix, the peak intensities of composites did not exhibit a consistent trend of augment or decrease.

Evaluation of the TG–MS curves of the α-Fe_2O_3/SR and γ-Fe_2O_3/SR samples

Figures 4 and 5 demonstrate the evolution of prominent volatiles from the α-Fe_2O_3/SR sample and the γ-Fe_2O_3/SR sample, respectively. The two samples contain α-Fe_2O_3 and γ-Fe_2O_3 and both showed no remarkable variation in T_0. But on the other hand, the peak intensity of the products from the side methyl degradation (both oxidation and bond breaking) showed a significant decrease. Comparing the α-Fe_2O_3/SR sample to the blank sample, peak intensity of methanol and methanoic acid decreased by 34.24 and 30.90 %, respectively, and peak intensity of methane also decreased by 8.47 %.The γ-Fe_2O_3/SR sample has an even better performance. Peak intensity of methanol and methanoic acid decreased by 40.22 and 35.39 %, respectively, and peak intensity of methane decreased by 24.03 %.

From the data, it can be seen directly that the characteristic products of the degradation of side methyl, especially methanol and methanoic acid, remarkably decreased with the addition of Fe_2O_3. This may be attributed to the effect of free radicals catching of Fe_2O_3, which inhibited the oxidation of the side methyl. In this regard, γ-Fe_2O_3 had a better performance. In our previous work [21], it was revealed that γ-Fe_2O_3 transformed into α-Fe_2O_3 gradually in the degradation process. γ-Fe_2O_3 had a spinel-type crystalline form which is unstable. In the degradation process, γ-Fe_2O_3 transformed into α-Fe_2O_3, and this process consumed oxygen [31, 32]. In this way, an oxygen-free region was formed surrounding the γ-Fe_2O_3 particles, which inhibited the oxidation of the side methyl. This may explain why γ-Fe_2O_3 had a better performance in the thermo-oxidative stability enhancement of SR comparing to α-Fe_2O_3.

Evaluation of the TG–MS curves of γ-Fe_2O_3 − CNTs/SR sample

Figures 6 and 7 show the evolution of prominent volatiles from the γ-Fe_2O_3 + CNTs/SR sample and the γ-Fe_2O_3 − CNTs/SR sample, respectively. Phenomena of T_0 augment and peak intensity decrease can both be observed in these two figures, which is evidence that these two samples both had effects of thermal conductivity enhancing and free radicals catching. However, with intensive study on them, conclusion can be drawn that the effects of them were not completely the same. In the degradation process of the γ-Fe_2O_3 + CNTs/SR sample, though T_0 showed an increment as the CNTs/SR sample do, the increment was much less than the CNTs/SR sample. It may be attributed to the relatively low content of CNTs in this sample, which leads to lower thermal conductivity of the composite. It can also be found that the effect of side methyl protection from oxidation and bond breaking was weaker than the γ-Fe_2O_3/SR sample, which was also caused by the lower content of γ-Fe_2O_3. The γ-Fe_2O_3 − CNTs/SR sample had same content of either CNTs or γ-Fe_2O_3 with the γ-Fe_2O_3 + CNTs/SR sample. However, the effect of protecting the side methyl from either oxidation or bond breaking was stronger than any other sample, which is confirmed by the changes in peak intensity of volatiles. In the degradation process of γ-Fe_2O_3 − CNTs/SR sample, peak intensity of methanol, methanoic acid and methane decreased greatly in a degree of 58.91, 57.25 and 27.45 %, respectively. This phenomenon can be explained by the synergistic effect of CNTs and Fe_2O_3.

Several reasons are displayed below to explain the synergistic effect between CNTs and Fe_2O_3 in thermal degradation process of SR. In our previous work [21], we have demonstrated that when attached to CNTs, the crystalline form of Fe_2O_3 was changed from α to γ. As mentioned above, γ-Fe_2O_3 had a better effect on thermo-oxidative stability of SR compared to α-Fe_2O_3, so the transformation of crystalline form has positive effect on SR matrix. Particle size is also one of the key factors that contribute to the intense synergistic effect. The particle size of γ-Fe_2O_3 is greatly reduced by the combination of CNTs [21], which can increase the specific surface area of γ-Fe_2O_3 to a large degree. In this way, the interaction between the γ-Fe_2O_3 particle and the SR matrix is greatly promoted, so the effect of free radical catching is greatly promoted. Another possible explanation is that the excellent electrical conductivity of CNTs may also form channels for electron transfer in redox reaction, which may accelerate the free radical catching process [33].

Conclusions

In this paper, TG–MS analysis was performed to make a further investigation on how different kinds of nanoparticles improved the thermo-oxidative stability of SR. Onset degradation temperatures of the samples containing CNTs (CNTs/SR, γ-Fe_2O_3 + CNTs/SR, γ-Fe_2O_3 − CNTs/SR) were all enhanced. This can be attributed to the extremely high intrinsic thermal conductivity of CNTs, which restrained overheating of each specific section, and thus, thermo-oxidative stability was improved. Methanol, methanoic acid and methane, which are characteristic products of the degradation of side methyl, all decreased in peak intensity with the addition of Fe_2O_3. This phenomenon can be explained by the effect of free radicals catching of Fe_2O_3. In this regard, γ-Fe_2O_3 did a better job than α-Fe_2O_3. This may be attributed to the transformation of crystalline form from γ-Fe_2O_3 to α-Fe_2O_3 in the

degradation process, which formed oxygen-free region surrounding the γ-Fe_2O_3 and restrained the oxidation of the side methyl. CNTs and Fe_2O_3 showed significant synergistic effect on thermal stability enhancement of SR. Sample containing γ-Fe_2O_3 − CNTs had the best performance in the prevention of side methyl from degradation, which can be seen from the remarkable decrease in methanol, methanoic acid and methane by 58.91, 57.27 and 27.45 %, respectively. Several reasons including transformation of crystalline form and reduced particle sizes are proposed to explain the synergistic effect.

Acknowledgements This investigation was supported by the National Natural Science Foundation of China (Grant No. 51273143).

References

1. Zhu M, Chung DDL. A three-dimensionally interconnected metal-spring network in a silicone matrix as a resilient and electrically conducting composite material. Composites. 1992;23:355–63.
2. Miwa M, Takeno A, Hara K, Watanabe A. Volume fraction and temperature dependence of mechanical properties of silicone rubber particulate/epoxy blends. Composites. 1995;26:371–7.
3. Genovese A, Shanks RA. Fire performance of poly(dimethyl siloxane) composites evaluated by cone calorimetry. Compos Part A Appl Sci Manuf. 2008;39:398–405.
4. Hanu LG, Simon GP, Cheng YB. Thermal stability and flammability of silicone polymer composites. Polym Degrad Stab. 2006;91:1373–9.
5. Guo J, Zeng X, Li H, Luo Q. Effect of curatives and fillers on vulcanization, mechanical, heat aging, and dynamic properties of silicone rubber and fluororubber blends. J Elastom Plast. 2012;44:145–63.
6. Liu YR, Huang YD, Liu L. Thermal stability of POSS/methylsiliconenanocomposites. Compos Sci Technol. 2007;67:2864–76.
7. Anyszka R, Bielniski DM, Pedzich Z, Szumera M. Influence of surface-modified montmorillonites on properties of silicone rubber-based ceramizable composites. J Therm Anal Calorim. 2015;119:111–21.
8. Zhu M, Chung DDL. Resilient composite of silicone and foamed tin as a new material for electrical and thermal contacts. Composites. 1991;22:219–26.
9. Wilson B, Ricardo FS, Fernando G. Interfacial reactions and self-adhesion of polydimethylsiloxanes. J Adhes Sci Technol. 1992;6:791–805.
10. Iijima S. Helical microtubules of graphitic carbon. Nature. 1991;354:56–8.
11. Kong J, Franklin NR, Zhou C, Chapline MG, Peng S, Cho K, et al. Nanotube molecular wires as chemical sensors. Science. 2000;287:622–5.
12. Park SJ, Bae KM, Seo MK. A study on rheological behavior of MWCNTs/epoxy composites. J Ind Eng Chem. 2010;16:337–9.
13. Jiang MJ, Dang ZM, Xu HP, Yao SH, Bai J. Effect of aspect ratio of multiwall carbon nanotubes on resistance-pressure sensitivity of rubber nanocomposites. Appl Phys Lett. 2007;91:072907.
14. Liu CH, Fan SS. Nonlinear electrical conducting behavior of carbon nanotube networks in silicone elastomer. Appl Phys Lett. 2007;90:041905.
15. Raza MA, Westwood AVK, Stirling C, Hondow N. Transport and mechanical properties of vapour grown carbon nanofibre/silicone composites. Compos Part A Appl Sci Manuf. 2011;42:1335–43.
16. Watts PCP, Fearon PK, Hsu WK, Billingham NC, Kroto HW, Walton DRM. Carbon nanotubes as polymer antioxidants. J Mater Chem. 2003;13:491–5.
17. Shen ZQ, Bateman S, Wu DY, Mcmahon P, Dell'Olio M, Gotama J. The effects of carbon nanotubes on mechanical and thermal properties of woven glass fibre reinforced polyamide-6 nanocomposites. Compos Sci Technol. 2009;69:239–44.
18. Lewicki JP, Liggat JJ, Patel M. The thermal degradation behaviour of polydimethylsiloxane/montmorillonite nanocomposites. Polym Degrad Stab. 2009;94:1548–57.
19. Lewicki JP, Liggat JJ, Pethrick RA, et al. Investigating the ageing behavior of polysiloxane nanocomposites by degradative thermal analysis. Polym Degrad Stab. 2008;93:158–68.
20. Hamdani S, Longuet C, Perrin D, et al. Flame retardancy of silicone-based materials. Polym Degrad Stab. 2009;94:465–95.
21. Li HY, Tao S, Huang YH, Su ZT, Zheng JP. The improved thermal oxidative stability of silicone rubber by using iron oxide and carbon nanotubes as thermal resistant additives. Compos Sci Technol. 2013;76:52–60.
22. Albis A, Ortiz E, Suárez A, Piñeres I. TG/MS study of the thermal devolatization of Copoazu peels. J Therm Anal Calorim. 2014;115:275–83.
23. Campostrini R, Abdellatief M, Leoni M, Scardi P. Activation energy in the thermal decomposition of MgH_2 powders by coupled TG–MS measureňments. Part 1. Comparison among TG- and MS- data processing. J Therm Anal Calorim. 2014;116:225–40.
24. Ksepko E, Labojko G. Effective direct chemical looping coal combustion with bi-metallic Fe-Cu oxygen carriers studied using TG-MS techniques. J Therm Anal Calorim. 2014;117:151–62.
25. Chang J, Fang YF. Quantitative analysis of accelerated carbonation products of the synthetic calcium silicate hydrate(C-S-H) by QXRD and TG/MS. J Therm Anal Calorim. 2015;119:57–62.
26. Camino G, Lomakin SM, Lazzari M. Polydimethylsiloxane thermal degradation Part 1. Kinet Asp Polym. 2001;42:2395–402.
27. Camino G, Lomakin SM, Legeard M. Thermal polydimethylsiloxane degradation Part 2. The degradation mechanisms. Polymer. 2002;43:2011–5.
28. Yu C, Shi L, Yao Z, Li D, et al. Thermal conductance and thermo-power of an individual single-wall carbon nanotube. Nano Lett. 2005;5:1842–6.
29. Moisala A, Li Q, Kinloch IA, Windle AH. Thermal and electrical conductivity of single- and multi-walled carbon nanotube-epoxy composites. Compos Sci Technol. 2006;66:1285–8.
30. Chua TP, Mariatti M, Azizan A, Rashid AA. Effects of surface-functionalized multi-walled carbon nanotubes on the properties of poly(dimethyl siloxane) nanocomposites. Compos Sci Technol. 2010;70:671–7.
31. Zboril R, Mashlan M, Petridis D. Iron(III) oxides from thermal processes synthesis, structural and magnetic properties, Mössbauer spectroscopy characterization, and applications. Chem Mater. 2002;14:969–82.
32. Tronc E, Chaneac C, Jolivet JP. Structural and magnetic characterization of ε-Fe_2O_3. J Solid State Chem. 1998;139:93–104.
33. Yu H, Quan X, Chen S, et al. TiO_2-multiwalled carbon nanotube heterojunction arrays and their charge separation capability. J Phys Chem C. 2007;111:12987–91.